Light in materials with periodic gain-loss modulation on a wavelength scale

Muriel Botey,[1] Ramon Herrero,[2] and Kestutis Staliunas[2,3]
[1]*Departament de Física i Enginyeria Nuclear, Urgell 187, ES-08036 Barcelona, Spain*
[2]*Departament de Física i Enginyeria Nuclear, Universitat Politècnica de Catalunya, Colom 11, ES-08222 Terrassa, Spain*
[3]*Institució Catalana de Recerca i Estudis Avançats, Pg. Ernest Lluch/Rambla Sant Nebridi, ES-08222 Terrassa, Spain*
(Received 23 March 2010; published 22 July 2010)

We analyze light-wave dynamics in artificial materials characterized by periodically modulated gain or loss on the wavelength scale. The study of the temporal dispersion in one-dimensionally modulated materials predicts mode-locked states and superluminal light propagation regimes in the parameter regions close to the locking regions. The study of spatial dispersion for a two-dimensional gain-loss modulation predicts nontrivial beam propagation effects such as self-collimation, angle-sensitive gain, and negative diffraction in such gain-loss-modulated materials.

DOI: 10.1103/PhysRevA.82.013828 PACS number(s): 42.70.Qs, 42.55.Tv, 42.25.Fx, 42.79.−e

I. INTRODUCTION

It is well known that light propagation through materials with periodically modulated indexes of refraction on the wavelength scale, the so-called photonic crystals (PCs), shows unusual properties. The best-known effects in PCs are related to modification of the temporal dispersion: the appearance of band gaps in the frequency domain and the subluminal propagation close to the band gaps [1]. The spatial propagation of monochromatic beams is also affected in PCs and results in recently discovered effects such as self-collimation [2], superrefraction [3], focalization [4], and spatial filtering [5] in at least two-dimensional (2-D) PCs, that is, in materials with a 2-D modulation of the refraction index.

Curiously, the seemingly analogous artificial materials, where not the refraction index but rather the gain-loss profile is periodically modulated on the wavelength scale, do not enjoy considerable attention compared with PCs, although such materials have become more and more technologically accessible [6]. The light propagation in gain-loss-modulated (GLM) materials has been studied only in the case of modulation in one spatial dimension (1-D), in relation with the so-called distributed feedback lasers [7]. Recently, wave dynamics in 1-D parity-time-invariant potentials has been considered [8], which are models for photonic systems with a combined gain and refraction index modulation. Only very recently, some of us initiated a study of the GLM for 2-D modulation [9], which even in the simplified paraxial approximation predicted interesting properties of beam propagation.

Here we initiate a systematic study of such 1-D and 2-D GLM artificial materials using the plane wave expansion (PWE) method as a basic tool. The PWE method is widely used to calculate the band structure of photonic crystals—here we adapt this method to the specifics of GLM materials. The method allows calculating the temporal and spatial dispersion curves as well as the angular gain profiles without any approximation and any restriction; that is, it is valid for modulation periods of the order of the wavelength since it is based on the full Maxwell equations.

First, we present the model based on the Maxwell equations with a modulated gain-loss function and derive the PWE model. Next, we perform an analytical treatment on a simple approximation (with one spatial dimension, truncated to two modes) and show the basic behavior reported. Finally, we make full plane wave expansions, calculate the band diagrams in both 1-D and 2-D cases, and prove the predicted effects: the mode locking and superluminal light dynamics for the 1-D case and beam self-collimation, angle-sensitive gain, and beam focalization for the 2-D case.

II. MODEL

We start from the wave equation as directly obtained from the Maxwell equations, which, in terms of the electric field, reads

$$\vec{\nabla}\times\vec{\nabla}\times\vec{E}=-\varepsilon(\vec{r})\frac{1}{c^2}\frac{\partial^2\vec{E}}{\partial t^2}. \tag{1}$$

Here $\varepsilon(\vec{r})$ is the relative electric susceptibility of the material, which consists of a real part (corresponding to the refractive index) and an imaginary part (corresponding to the gain or loss). In general, the ratio between the real and imaginary parts of such susceptibility depends on the materials and conditions. However, in order to report the basic effects, we restrict the analysis to the GLM case, where $\varepsilon(\vec{r})=1+im(\vec{r})$. We note that the effects reported persist also for a small modulation of the refractive index. Moreover, we consider here, without loss of generality, the case of balanced mean gain or loss: $\int m(\vec{r})d\vec{r}=0$. The general case (e.g., with gain) can be obtained from the balanced case by adding the corresponding net gain exponent.

We consider a 2-D modulation of the gain-loss profile and expand the susceptibility in terms of multiples of the two inverse lattice vectors $\vec{q}_1$ and $\vec{q}_2$. From Eq. (1), we directly obtain the equations for the expansion coefficients of the unipolarized electric field $E(\vec{r},t)=e^{-i\omega t+i\vec{k}\vec{r}}\sum_j\sum_l a_{jl}e^{i(j\vec{q}_1+l\vec{q}_2)\vec{r}}$:

$$a_{jl}\left[|\vec{k}+j\vec{q}+l\vec{q}|^2+\frac{\omega^2}{c^2}\right]=-i\frac{\omega^2}{c^2}\sum_p\sum_s a_{j-p,l-s}m_{ps}, \tag{2}$$

which is the main system of equations to be solved. We note that Eq. (2) is analogous to the PWE for PCs; however, the coupling coefficients are imaginary in the case of GLM materials.

The solvability condition of Eq. (2) allows us to calculate the dispersion relations: $\omega(k)$. As the coupling coefficients in Eq. (2), contrary to the PC case, are not real valued, the coupling matrix is non-Hermitian, and the eigenvalues of the problem are not necessarily real valued. The real parts of the eigenfrequencies, as in the case of PCs, correspond to the frequencies of the Bloch modes, and the imaginary part of the frequency is the net gain or loss of the corresponding Bloch mode.

III. TWO-MODE CASE

Before starting the numerical study of the complex dispersion in 1-D and 2-D, let us get some insight into what can be expected by maximally simplifying Eq. (2), that is, by only retaining two interacting modes. This case can be mathematically rigorously derived from Eq. (2) for a 1-D harmonic and weak gain-loss modulation: $m(\vec{r}) = m_0 \cos(qx)$, expanding by smallness parameter $|m_0| = O(\varepsilon), \varepsilon \ll 1$. Close to degeneracy point $k_0 = q/2$, the amplitudes a_0 and a_1 of the field components with propagation wave vectors $\vec{k}$ and $\vec{k} - \vec{q}$ fulfill

$$\left(\Delta k - \frac{\Delta\omega}{c}\right) a_0 - i\frac{m_0 k_0}{2} a_1 = 0, \tag{3a}$$

$$\left(-\Delta k - \frac{\Delta\omega}{c}\right) a_1 - i\frac{m_0 k_0}{2} a_0 = 0, \tag{3b}$$

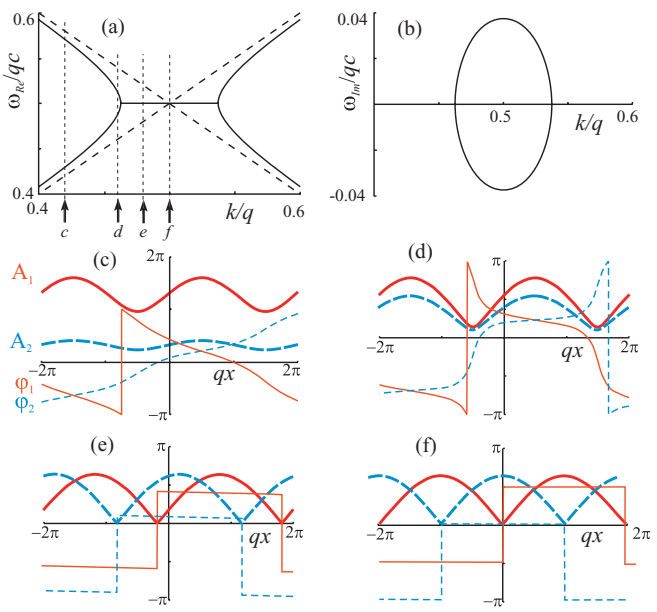

FIG. 1. (Color online) (a) Dispersion curves (real part of the frequency) and (b) gain-loss profiles (imaginary part of the frequency) at the vicinity of the cross-point of the dispersion curves of two dissipatively coupled eigenmodes (the dispersions of uncoupled modes are shown by the dashed lines). The parameters used are $q = 1$ and $m_0 = 0.15$.(c–f) Mode modulus A (bold line) and phase φ (thin line) of the two eigenmodes (solid and dashed lines) for different parameters for $k/q = 0.42$; $k/q = 0.46$, that is, in unlocked area but close to the locking boundary ($k_l = k_0 - m_0 k_0/2 = 0.426q$); $k/q = 0.48$; and $k/q = 0.5$, that is, at the middle of the locking area, respectively.

where $\Delta k = k - k_0$ and $\Delta\omega = \omega - \omega_0$ ($\omega_0 = qc/2$) are deviations from the degeneracy point.

The set of equations (3) has a simple analytic solvability condition:

$$\Delta\omega = \pm c\sqrt{\Delta k^2 - \frac{m_0^2 k_0^2}{4}}, \tag{4}$$

which is the temporal dispersion curve, as represented in Figs. 1(a) and 1(b). It differs crucially from those typically appearing in the theory of PCs: the dispersion curves of the uncoupled modes (dashed curves) do not "push" mutually and do not form the band gap around their cross-points but rather pull one another and lock to some common frequency. The width of the locking area is $m_0 q/2$, as follows from Eq. (4), and the maximal net gain that takes place for $\Delta k = 0$ is $\omega_{\mathrm{Im}} = c m_0 q/4$. Two different Bloch modes exist for each k, as shown in Figs. 1(c)–1(f). At the degeneracy point, the intensity profiles of the corresponding Bloch modes are mutually shifted by a half period: The maxima of the field intensity of the amplifying (decaying) mode falls into the gain (loss) region of the gain-loss profile [see Fig. 1(f)]. The phase shift between Bloch modes decreases moving away from the degenerated point. We note [see also Fig. 1(e)] that the Bloch modes are not orthogonal in all the mode-locking area (except for at the degeneracy point).

We note that outside but close to the locking region, the dispersion curves are strongly tilted, with the local slopes approaching infinity at the boundary of the locking area. This means that the light propagation (in a group velocity sense) becomes superluminal for particular frequencies. The eigenmodes present steep phase variations in a stairwise manner close to the boundary of the locking area [see Fig. 1(d)] and smoothly far away from the boundary [Fig. 1(c)]. Inside the locking region, the phase makes π jumps, indicating formation of standing waves [Fig. 1(e)].

The described behavior is universal at the vicinity of the cross-point of two dispersion curves, when the coupling between the modes is of dissipative character. The coupling of modes in GLM materials is indeed dissipative, in contrast to the reactive coupling of modes in the case of PCs, as follows from Eq. (2). Next, we check this generic mode interaction figure with the full PWE method, that is, without any simplifications or approximations.

IV. ONE-DIMENSIONAL GLM

We used stepwise gain-loss geometry, as illustrated in the inset in Fig. 2. We took care that the net gain was equal to zero; therefore we chose equal gain and loss in two subsequent layers. The dispersion diagram, including the lowest four photonic bands, is shown in Fig. 2.

The dissipative coupling of modes, as expected, results in mode-locking areas (instead of band gaps, as in the PC case). The width of the corresponding mode-locked regions corresponds well to the value evaluated analytically in the two-mode approximation, that is, to the corresponding coefficient in the harmonic expansion of the gain-loss profile m_i. For example, the locking between the first and second photonic bands follows from m_1, the locking region between the third and fourth bands follows from m_3, and so forth. The locking

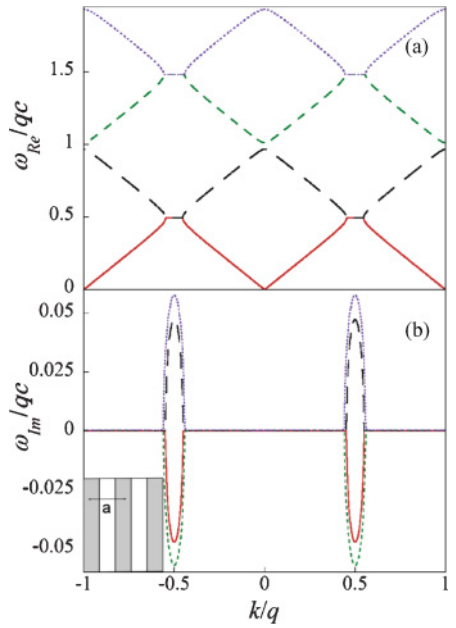

FIG. 2. (Color online) Dispersion curves of a 1-D GLM material consisting of alternating layers of gain $m = -0.3$ and loss $m = 0.3$ of equal length, $a/2$, as shown in the inset. (a) Real part of the frequency of the first four Bloch modes. (b) Imaginary part of the frequency of the same modes. Calculations are obtained by PWE using 1001 plane waves. Frequency is expressed in reduced ω/qc units, where q is $2\pi/a$.

between the second and third bands does not occur for the particular gain-loss profile chosen (where the gain and loss areas are of equal thickness) since $m_2 = 0$.

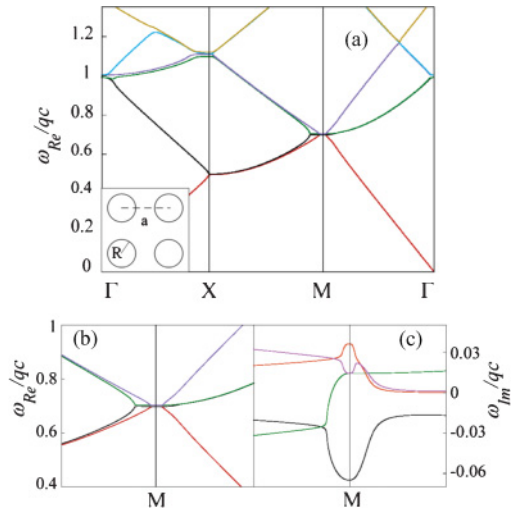

FIG. 3. (Color online) Dispersion curves of a 2-D GLM consisting of a square lattice of lossy cylinders of radius R, separated by a distance a, embedded in a background medium with gain; see the inset. (a) Real part of the frequency of the lowest six modes in TM polarization. (b) M point zoom with the first four modes. (c) Imaginary part of the frequencies of the modes depicted in (b). Calculations are obtained by PWE using 361 plane waves in the expansion. The parameters used are as follows: loss $m = 0.3$ for the cylinders, gain otherwise $m = -0.118$, $R = 0.3a$ (balanced gain and loss). Frequency is in terms of ω/qc.

V. TWO-DIMENSIONAL GLM

We considered a periodic lattice of circular areas of gain, with a square symmetry, as illustrated in the inset in Fig. 3. The lossy cylinders are embedded in a background with gain which is chosen to preserve zero mean net gain in the unit cell of the crystal. The band diagram, including the lowest six Bloch modes, is shown in Fig. 3. We adapt the conventions from the theory of 2-D photonic crystals; that is, we plot the eigenfrequencies along the ΓXMΓ path. We chose TM polarization; however, we note that TE polarization leads to qualitatively similar mode-locking behavior.

The basic picture in the 2-D case is that the modes with the wave vectors lying at the boundaries of the Brillouin zones

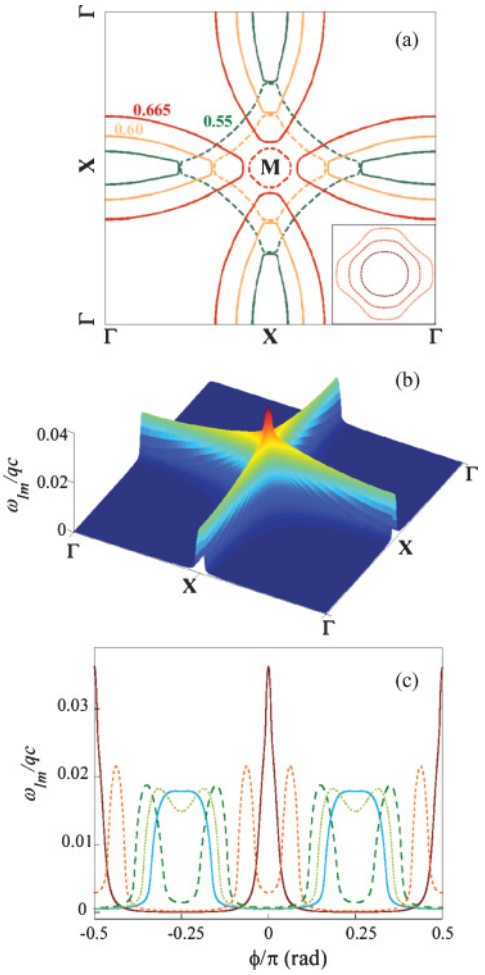

FIG. 4. (Color online) (a) Two-dimensional plot of the isofrequency lines of two lowest Bloch modes for 2-D GLM, as described in Fig. 3. The doted curves display the first Bloch mode and the solid curves display the second Bloch mode. The isolines correspond to real reduced frequency values of $\omega_{\mathrm{Re}}/qc = 0.55, 0.60, 0.665$ (where the latter is the self-collimation frequency). The inset shows the isofrequency lines of the first Bloch mode for $\omega_{\mathrm{Re}}/qc = 0.65, 0.665, 0.68$, corresponding to negative, zero, and positive diffraction, respectively. (b) Gain-loss profile (imaginary part of the reduced frequency) of the first Bloch mode. (c) Angular gain profile of the lower order mode for three values of the wavevector modulus: $0.5q$ (solid blue curve), $0.51q$ (dotted green curve), $0.525q$ (long-dashed green curve), $0.6q$ (short-dashed orange curve), and $\sqrt{2}q/2$ (red solid curve).

mutually lock and that the net amplification occurs in the locking regime. The effect is extremely strong at the edges of the Brillouin zones, where several (in our case four) modes are in resonance, and lock to a common frequency, as shown in Fig. 3(b). This means that the gain becomes highly directional and is concentrated around particular angles corresponding to the symmetry directions of the structure.

Figure 4 represents a complete 2-D plot of the frequency as well as of the gain profile for the lowest Bloch modes in the area around the corner of the Brillouin zone. The isofrequency lines belonging to the first and second photonic bands nearly touch one another; that is, different from the case of PCs, no angular band gaps appear.[1] The angular gain area shows a sharp peak, which means that radiation with a particular frequency, represented by the isofrequency line crossing the corner of the Brillouin zone, shows a high angular directionality of the gain. The radiation on the other, higher or lower frequencies shows two high-gain regions placed symmetrically with respect to the diagonal direction M [Fig. 4(c)]. We note that the spatial dispersion curves $k_{||}(k_{\perp})$ can become straight between the areas of high gain, which indicates self-collimation [inner dotted line in Fig. 4(a)], or even convex, which indicates negative diffraction [inset in Fig. 4(a)]. The latter case can result in focalization of the beam behind the GLM media.

VI. CONCLUSIONS

We considered 1-D and 2-D modulations of the gain-loss profile on the wavelength scale and calculated the dispersion characteristics of the system. The general result is drastically different from that in PCs: Whereas in PCs, the interaction deforms the dispersion so that there appear well-known band gaps, in the case of GLM, the band gaps do not appear, but instead, frequency-locked areas do. The dispersion curves, either temporal or spatial, deform therefore in a different way than in PCs. As a result, in 1-D GLMs appear superluminal regimes (in PCs, subluminal). In 2-D cases, similar to photonic crystals, also self-collimation regimes appear. However, unlike photonic crystals, in the 2-D GLM case, highly directional gain is possible. In our investigated geometries, the high-gain directions are along the diagonals of the square lattice.

We note one more interesting result following from the isolines in 2-D (Fig. 4): The isofrequency lines close to the maximum angular gain area can develop positive or negative curvatures [see Fig. 4(a)]. The case of positive curvature (frequency slightly larger than that of self-collimation frequency) is especially interesting as the positive curvature corresponds to negative diffraction. This means that the radiation with corresponding frequencies, after amplification in the GLM, can focalize behind. This effect can be of large technological importance and is to be investigated separately.

We did not calculate the band diagrams in 3-D; however, the main conclusions are expected to remain: the appearance of narrow-gain areas around the corners of the 3-D Brillouin zone.

[1] The isofrequency lines of the neighboring bands touch when two modes are interacting (at the boundaries of the Brillouin zone), in accordance with Eq. (4) At the corners of the Brillouin zone, where several modes are in resonance and in efficient interaction, a small split is observed–the effect is beyond the scope of the present study.

ACKNOWLEDGMENTS

The work is financially supported by Spanish Ministerio de Educación y Ciencia and European FEDER through Project No. FIS2008-06024-C03-02 and by COST Action No. MP0702 from the European Community.

[1] E. Yablonovitch, Phys. Rev. Lett. **58**, 2059 (1987); S. John, *ibid.* **58**, 2486 (1987).

[2] H. Kosaka *et al.*, Appl. Phys. Lett. **74**,1212 (1999); D. N. Chigrin *et al.*, Opt. Express **11**, 1203 (2003); R. Illiew *et al.*, Appl. Phys. Lett. **85**, 5854 (2004); D. W. Prather *et al.*, Opt. Lett. **29**, 50 (2004); K. Staliunas and R. Herrero, Phys. Rev. E **73**, 016601 (2006).

[3] A. Lupu *et al.*, Opt. Express **14**, 2003 (2006); J. J. Baumberg *et al.*, Appl. Phys. Lett. **85**, 354 (2006); T. Prasad *et al.*, Phys. Rev. B **67**, 165103 (2003).

[4] S. Savo *et al.*, Opt. Express **17**, 19848 (2009); Q. Wu *et al.*, J. Opt. Soc. Am. B **23**, 479 (2006); X. Wang *et al.*, Opt. Express **12**, 2919 (2004).

[5] K. Staliunas and V. J. Sánchez-Morcillo, Phys. Rev. A **79**, 053807 (2009).

[6] F. Chen *et al.*, Opt. Express **16**, 16746 (2008); R. Oulton *et al.*, *ibid.* **15**, 17221 (2007); I. S. Nikolaev, P. Lodahl, and W. L. Vos, Phys. Rev. A **71**, 053813 (2005); M. Hiroaki *et al.*, Opt. Express **16**, 13676 (2008).

[7] H. Kogelnik and C. V. Shank, J. Appl. Phys. **43**, 2327 (1972); H.-P. Tong *et al.*, Opt. Express **18**, 2613 (2010); C. Ye *et al.*, *ibid.* **15**, 936 (2007).

[8] K. G. Makris, R. El-Ganainy, D. N. Christodoulides, and Z. H. Musslimani, Phys. Rev. Lett. **100**, 103904 (2008); S. Longhi, *ibid.* **103**, 123601 (2009); Phys. Rev. A **81**, 022102 (2010).

[9] K. Staliunas, R. Herrero, and R. Vilaseca, Phys. Rev. A **80**, 013821 (2009).